ACS Sustainable Chemistry & Engineering

Research Article

Cite This: ACS Sustainable Chem. Eng. 2018, 6, 13078−13085

pubs.acs.org/journal/ascecg

Fungal Glutathione Transferases as Tools to Explore the Chemical Diversity of Amazonian Wood Extractives

Thomas Perrot,[†,∥] Mathieu Schwartz,[‡,∥] Fanny Saiag,[†] Guillaume Salzet,[†] Stéphane Dumarçay,[§] Frédérique Favier,[‡] Philippe Gérardin,[§] Jean-Michel Girardet,[†] Rodnay Sormani,[†] Mélanie Morel-Rouhier,[†] Nadine Amusant,[⊥] Claude Didierjean,[‡] and Eric Gelhaye*[,†]

[†]Université de Lorraine, INRA, IAM, F-54000 Nancy, France

[‡]Université de Lorraine, CNRS, CRM2, F-54000 Nancy, France

[§]Université de Lorraine, INRA, LERMAB, F-54000 Nancy, France

[⊥]CIRAD, UMR Ecofog (AgroParisTech, CIRAD, CNRS, INRA, UA), BF701−97310 Kourou, Cedex, France

Supporting Information

ABSTRACT: The natural durability of wood is linked to its chemical composition and in particular the presence of metabolites called extractives that often possess chemical reactivity. For dealing with these compounds, wood degraders have developed detoxification systems usually involving enzyme families. Among these enzymes, glutathione transferases (GSTs) are involved in the decrease of the reactivity of toxic compounds. In this study, the hypothesis that the detoxification systems of wood decaying fungi could be indicators of the chemical reactivity of wood extracts has been tested. This approach has been evaluated using 32 wood extracts coming from French Guiana species, testing their antimicrobial ability, antioxidative properties, and reactivity against six GSTs from the white rot *Trametes versicolor*. From the obtained data, a significant correlation between the antimicrobial and antioxidative properties of the tested wood extracts and GST interactions was established. In addition, the chemical analysis performed on one of the most reactive extracts (an acetonic extract of *Bagassa guianensis*) has demonstrated oxyresveratrol as a major constituent. We were able to cocrystallize one GST with this commercially interesting compound. Taken together, the presented data support the hypothesis that detoxifying enzymes could be used to identify the presence of molecules of industrial interest in wood extracts.

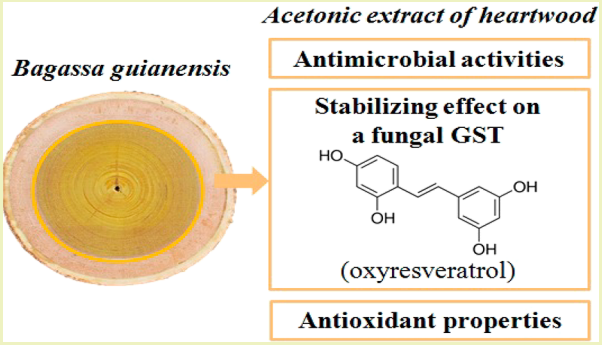

KEYWORDS: *Trametes versicolor, Amazonian wood species, Bagassa guianensis, Glutathione transferase, Stilbene*

INTRODUCTION

Wood is a major renewable resource with many fields of application as energy, building, or polymers production. Beyond the presence of structural polymers (cellulose, hemicellulose, and lignin), wood also contains secondary metabolites called extractives. The chemical composition of extractives is various and includes terpenes, fatty acids, simple phenols, flavonoids, tannins, and stilbenes. Although the functions of these wood molecules often remain unclear, they usually possess properties of interest such as antimicrobial and antioxidative activities.[1,2] Because of their properties, these compounds could be used for several industrial purposes in particular for wood preservation, crop protection, medicinal treatments, or cosmetics.[3] However, they could also be a problem for lignocellulosic biomass valorization, limiting its enzymatic digestibility.[4]

The diversity and the potential toxicity of these extractives suggest that wood degraders and in particular wood decaying fungi are adapted to the presence of these potential toxic molecules.[5] Beyond their extracellular systems, which allow them to degrade lignocellulosic substrates,[6,7] wood-decaying fungi indeed possess extended detoxifying enzyme families, such as cytochrome P450 monooxygenases (P450s) and glutathione transferases (GSTs).[5] Such extensions are also found in herbivorous insects with these multigenic families playing key functions in the detoxification of plant defense chemicals and also in the evolution of metabolic resistance to chemical insecticides.[8] Concerning GSTs, their activity or even their expression are widely used to evaluate physiological and environmental stress of diverse organisms from molluscs to humans.[9−11] In wood-decaying fungi, the extension of the GST family concerns mainly specific phylogenetically based classes named Ure2p, GST Omega (GSTO), and GSTFuA.[12−14] GSTFuA is able to cleave lignin β-O-4 aryl ether bond in the white-rot fungus *Dichomitus squalens*.[15] In addition, GSTOs from *Trametes versicolor* interact with wood extracts from

Received: June 5, 2018
Revised: July 31, 2018
Published: August 25, 2018

Downloaded via CIRAD on January 15, 2019 at 14:37:15 (UTC).
See https://pubs.acs.org/sharingguidelines for options on how to legitimately share published articles.

© 2018 American Chemical Society

DOI: 10.1021/acssuschemeng.8b02636
ACS Sustainable Chem. Eng. 2018, 6, 13078−13085

temperate forest[16] and more particularly with polyphenols such as hydroxylbenzophenones and flavonoids.[17] In this context, we postulated that GSTs could be used as tools to identify wood extracts that possess interesting biological properties. To test this hypothesis, we investigated the biochemical interactions between six GSTOs from *Trametes versicolor*[16] and an environmental collection of wood extracts. *Trametes versicolor* is common and widespread in boreal and temperate northern hemisphere and also occurs in tropical areas of both hemispheres.[18] The six studied GST isoforms, which contain a serinyl residue in the active site, belong to the fungal type-III Omega class. The tridimensional structures of two of them, TvGSTO3S and TvGSTO6S, have been recently solved.[17] The extracts came from French Guiana woody species known to be naturally durable against fungi.[1,2,19] Using high-throughput biochemical methods, we show here that the chemical interactions of one isoform with the tested wood extracts are highly correlated with the chemical and biological properties (antioxidative and antimicrobial activities) of these compounds. Additional biochemical and structural experiments demonstrated the interactions between TvGSTO2S and oxyresveratrol, a stilbene largely used by the cosmetics industry, supporting the feasibility of our approach.

EXPERIMENTAL SECTION

Chemicals. The solvents used for the extraction step and for the chromatographic fractionation by HPLC are provided from Honeywell and Carlo Erba, respectively.

Wood Extracts. Heartwoods from *Peltogyne venosa*, *Dicorynia guianensis*, *Bagassa guianensis*, *Hymenaea courbaril*, *Tabebuia serratifolia*, *Sextonia rubra*, *Andira coriacea*, and *Eperua falcata* were from commercial origin (Degrad Saramaca's sawmill, Kourou, French Guiana). All species are well known and used in the building industry because of their durability against wood-rotting fungi (i.e., with natural durability against fungi rated 1−3 on a scale of 5 with class 1 being the most durable).

Each conditioned sample (12% relative humidity) was ground to fine sawdust with particle size between 0.2 and 0.4 mm before extraction. The obtained sawdust was Soxhlet-extracted successively during 24 h using the following solvents: dichloromethane, acetone, toluene/ethanol (2/1, v/v), and water. After each extraction, organic solvents were evaporated under vacuum using a rotary evaporator. Dried extractives were stored in a freezer (−18 °C) before analyses.

Chromatographic Analysis of the *Bagassa guianensis* Heartwood Acetonic Extract. *Bagassa guianensis* heartwood acetonic extract was fractioned by reverse chromatography (Shimadzu Prominence HPLC system) as previously described.[17] Twelve injections of 80 μL of the extract at 92 mg mL^{-1} were fractioned onto a Kinetex Biphenyl column (250 × 4.6 mm internal diameter, 5 μm particle size, 10 nm porosity; Phenomenex) previously equilibrated in water containing 0.1% formic acid. A linear gradient of methanol from 0 to 100% in the presence of 0.1% formic acid was applied for 45 min at 1 mL min^{-1}. Collected fractions (1 mL) were dried using a vacuum centrifuge concentrator SpeedVac (UniEquip) and then solubilized in 1 mL of dimethyl sulfoxide (DMSO).

Chemical Characterization of the Wood Extracts. Gas chromatography coupled to mass spectrometer (GC-MS) allowed the identification and relative quantification of the different substances present in the wood extracts. Samples were analyzed as trimethylsilyl derivatives using the following procedure. In a screw-capped vial, a sample of ∼1 mg of dry extract was dissolved in 100 μL of BSTFA/TMCS 1% (N,O-Bis(trimethylsilyl)trifluoroacetamide with 1% of trimethylsilyl chloride from Sigma-Aldrich). The solution was vortexed-stirred for ∼1 min and heated at 70 °C for 20 h. After evaporation of the silylating reagent, the residue was diluted in 1 mL of ethyl acetate. Silylation is performed to ensure as far as possible the extractives thermal stability in the gas-chromatography temperature conditions, mainly to avoid any decomposition or dehydration side-reactions possibly occurring when hydroxyl groups are free. The GC-MS analysis was performed on a Clarus 600 GC gas chromatograph coupled to a SQ8 mass spectrometer (PerkinElmer). Separation was carried out on a 5% diphenyl/95% dimethyl polysiloxane fused-silica capillary column (J&W Scientific DB-5MS, 30 m × 0.25 mm × 0.25 μm). The injection was performed at 250 °C in the splitless mode with helium as carrier gas at a constant flow of 1 mL min^{-1}. Chromatographic conditions were as follows: initial temperature 80 °C, 2 min isothermal conditions, 10 °C min^{-1} to 190 °C, 15 °C min^{-1} to 280 °C, 10 min isothermal conditions, 10 °C min^{-1} to 300 °C, 14 min isothermal conditions. The component ionization was performed by electron impact (70 eV ionization energy) to achieve their identification by mass spectra comparison with the NIST library. Samples relative compositions in extractives were obtained by the area of each peak determined on the total ion current (TIC) chromatogram divided by the sum of all of the detected peak areas.

Glutathione Transferases. GSTs that belong to the omega class have been heterogeneously produced using synthetic genes as described in Deroy et al.[16] The synthetic genes have been designed from the sequenced genome and transcriptomic studies of the white-rot *Trametes versicolor* from the following genes: TvGSTO1S, whose accession number in the JGI database is Tv75639; TvGSTO2S: Tv56280; TvGSTO3S: Tv48691; TvGSTO4S: Tv65402; TvGSTO5S: Tv54358; TvGSTO6S: Tv23671.[17]

Fluorescence-Based Thermal Stability Assay. This assay was performed as described in Deroy et al.[16] The denaturation temperature (T_d), which corresponds to the temperature where the protein is 50% unfolded, was determined using the first derivative of the obtained data in the presence or absence of potential ligands. As reference, experiments were conducted by adding DMSO only, allowing the determination of T_d ref. Then, the difference between the denaturation temperature of the protein incubated with wood extracts and with DMSO only (T_d ref) were calculated to obtain the thermal shift (ΔT_d). The sum of the absolute values of ΔT_d of the six TvGSTOS studied, $\Sigma\Delta T_d$, was determined for each wood extract.

Inhibition Kinetics. Glutathione transferase activity of TvGSTO2S (10 nM) has been tested using phenethyl isothiocyanate (PEITC) (25−250 μM) and reduced glutathione (GSH) (1 mM) in 100 mM phosphate buffer pH 6.4. The appearance of the glutathionylated product was followed measuring the absorbance at 274 nm in the presence and absence of oxyresveratrol. The catalytic constants (k_{cat}, K_M, and K_I) were calculated using the GraphPad software with the nonlinear regression based on the Michaelis−Menten model and the mixed model inhibition.

Real-Time Molecular Interaction Study. The binding of oxyresveratrol onto TvGSTO2S was investigated in real-time with an MPC-48-2-R1-S biochip placed in a biosensor analyzer switchSENSE DRX (Dynamic Biosensors GmbH, Planegg, Germany) available at the ASIA platform (Université de Lorraine). The GST was solubilized at 200 nM in 10 mM sodium phosphate buffer, pH 7.4, containing 40 mM NaCl, 0.05% Tween20, 50 μM EDTA, and 50 μM EGTA (PE40 buffer). The chip is composed of four independent channels, each containing six electrodes (for more information, see Langer et al.).[20] Real-time measurements of kinetics responding to changes to the molecular environment upon analyte binding (oxyresveratrol) gave the association kinetics (k_{on}) of the interaction. Oxyresveratrol at 100 μM in PE40 buffer containing 2% DMSO was injected in the fluidic at 5 μL min^{-1} for 5 min to a chosen channel of the chip (association kinetics), and then PE40 buffer containing 2% DMSO was injected at 50 μL min^{-1} for 30 min (dissociation kinetics). The real-time measurements were determined at 25 °C. Slight release of the GST from the dsDNAs was observed when only buffer was injected in the fluidic, and the corresponding signal was subtracted to normalize the signal of the interaction. All curves were analyzed by nonlinear fitting of single-exponential functions with the switchANALYSIS software from Dynamic Biosensors.

Microbial Growth. The growth of *Phanerochaete chrysosporium* RP78 (genome available on the Web site of the Joint Genome Institute, https://genome.jgi.doe.gov/Phchr2/Phchr2.home.html) has

DOI: 10.1021/acssuschemeng.8b02636
ACS Sustainable Chem. Eng. 2018, 6, 13078−13085

been followed by laser nephelometry.[21] For inoculum preparation, spores were collected from 8 day old solid cultures by adding broth followed by gentle scraping of the agar plates. The wells of the microplates were filled as previously.[22] Growth was automatically recorded for ≥30 h at 37 °C using a nephelometric reader (NEPHELOstar Galaxy, BMG Labtech, Offenburg, Germany). The maximal growth rates (μ_{max}) were determined from the growth curves measuring the maximal slope as described by Joubert et al.[21]

The bacterial strains *Collimonas pratensis* Ter91 and *Burkholderia fungorum* LMG 16225 have been isolated from *Phanerochaete chrysosporium* mycosphere during a microcosm experiment on beech.[23,24] Growth was automatically recorded for ≥48 h at 25 °C using a nephelometric reader. The growth rates have been determined from the growth curves measuring the maximal slope during the exponential phase.

The growth of *Saccharomyces cerevisiae* (strain 23344C) was studied in the presence of fractions from the acetonic extract of *Bagassa guianensis*. For each fraction, the growth tests have been performed in 198 μL of culture of *S. cerevisiae* in liquid YPD medium (Yeast, Peptone, and D-glucose). Two microliters of fraction was added to the culture, and the growth was analyzed by following the turbidimetry at 600 nm during 36 h (one read per 30 min). A control condition by testing the effect of the solvent (2 μL of DMSO) was also performed.

The inhibition index (I) of the microbial growth was calculated using the formula $I = 1 - (\mu_{max}/\mu_{max}\text{control})$ (1), where μ_{max} and μ_{max}control correspond to the maximal growth rate obtained in the presence and absence of wood extracts, respectively.

Antioxidative Properties. *Reducing Power Activity.* To determine the reducing activity of each wood extract, the method of Oyaizu[25] and Yen and Chen[26] was used as described in Canabady-Rochelle et al.[27] The reducing power is expressed according to a calibration curve based on the using of ascorbic acid (equivalent of ascorbic acid in μg L^{-1}).

Phenolic Content. Total phenolic content of the tested wood extract was estimated using the Folin−Ciocalteu method adapted to a 96-well microplate.[28] The absorbance was measured at 735 nm by using a microplate reader (EnSight Multimode Plate Reader, PerkinElmer). The phenolic content is expressed according to a calibration curve based on the use of gallic acid (equivalent of gallic acid in μg L^{-1}).

Statistical Analysis. All statistical analysis including Pearson correlations between variables, principal component analysis, ANOVA, and Tukey's test have been obtained from the XLSTAT software (XLSTAT 2017 Microsoft Excel, Addinsoft, France, 2017). For performing the Pearson correlations, the antimicrobial properties were represented by the inhibition index (I, as described above); the absolute values of thermal shifts ($|\Delta T_d|$) were required, and the values of the phenolic content and reductase activity were not modified (corresponding to equivalents of gallic acid and ascorbic acid in μg L^{-1}, respectively). These data have been also used for the principal component analysis.

Crystallographic Study. *Crystallogenesis.* A first screening of 288 crystallization conditions was carried out at the CRM² crystallogenesis platform (Université de Lorraine) by using the vapor diffusion method with an Oryx 8 crystallogenesis robot (Douglas Instrument). Crystals were optimized in Linbro plates using the hanging-drop method at 4 °C. The best crystals of TvGSTO2S were obtained by mixing 1 μL of protein (18 g L^{-1}) with 0.2 μL of crystal seed stock (prepared by crushing small crystals obtained during the screening step) and 1 μL of a solution containing 10.7% PEG 4000, 0.1 M HEPES-MES buffer at pH 7.0 (at a ratio of 4:6, respectively), 0.05 M sodium acetate, and 0.05 M magnesium chloride. The reservoir contained 1 mL of the same crystallization condition. Crystals of TvGSTO2S−oxyresveratrol complex were prepared by the "dry soaking method" as explained previously.[17] Briefly, 0.1 μL of commercial oxyresveratrol (100 mM in DMSO) was deposited on a cover slide and left to complete evaporation. Then, 1 TvGSTO2S crystal together with 1 μL of its mother liquor was dispensed on the dried oxyresveratrol. After one-day incubation, the crystal did not show any damage and was flash frozen after a quick soaking in its mother liquor supplemented with 20% glycerol.

Data Collection, Processing, and Refinement. Preliminary X-ray diffraction experiments were carried out in house on an Agilent SuperNova diffractometer (Oxford Diffraction) equipped with a CCD detector. Data collections were carried out at the ESRF on beamline FIP BM30A (Grenoble, France). TvGSTO2S crystals diffracted up to 2.19 Å. Data sets were indexed and integrated with XDS[29] and scaled and merged with Aimless from the CCP4 suite.[30] The structure of TvGSTO2S was solved by molecular replacement using MOLREP with the coordinates of *Trametes versicolor* GSTO3S (PDB ID: 6F43) as the search model. A file of restraints for oxyresveratrol was generated with the GRADE server (http://grade.globalphasing.org/cgi-bin/grade/server.cgi). Structures were refined with PHENIX[31] and manually improved with COOT.[32] Validation of all structures was performed with MolProbity[33] and the PDB validation service (http://validate.wwpdb.org). Coordinates and structure factors have been deposited in the Protein Data Bank under accession IDs 6GIB and 6GIC.

RESULTS

Interactions between Wood Extracts and TvGSTOs. Heartwoods of *Peltogyne venosa*, *Dicorynia guianensis*, *Bagassa guianensis*, *Hymenaea courbaril*, *Tabeuia serratifolia*, *Sextonia rubra*, *Andira coriacea*, *Eperua falcata*, and *Eperua grandiflora* have been sequentially extracted using four solvents exhibiting different polarities (dichloromethane, acetone, toluene/ethanol, and water). The interactions between the 32 obtained wood extracts and the six GSTs from *Trametes versicolor* were studied using the thermal shift assay (TSA), a high-throughput ligand-screening method based on the modification of protein thermal denaturation. Along a gradient of temperature, the denaturation is followed by monitoring fluorescence enhancement of a probe (SYPRO Orange) that binds to protein hydrophobic patches upon denaturation process. This TSA method has been successfully used to detect interactions between proteins and libraries of molecules.[16,17] The shift of the thermal denaturation temperature (ΔT_d) induced by the tested wood extract dissolved in DMSO was measured in comparison to a control performed with pure DMSO. Each enzyme displays a specific pattern of interactions with the tested extracts (Table S1). The interactions between each isoform and the tested extracts are not significantly related to the extraction solvent used (Tukey's test, $p > 0.05$). Nevertheless, the global reactivity of the six isoforms, named $\Sigma|\Delta T_d|$ (corresponding to the sum of the absolute values of ΔT_d, which have been measured for all isoforms), was significantly correlated to the polarity of the used solvent. The dichloromethane extracts indeed induced a significantly higher $\Sigma|\Delta T_d|$ than the other extracts (Tukey's test, $p = 0.015$), suggesting that the hydrophobic compounds extracted with this solvent have a significant effect on the thermal stability of the GSTs. As shown for *Eperua falcata* dichloromethane extract, these hydrophobic molecules could increase or decrease the thermal denaturation temperature depending on the considered proteins. This extract indeed decreased the thermal stability of TvGSTO3S (ΔT_d = −7.5 °C) and TvGSTO5S (ΔT_d = −2.1 °C) and had a positive effect on the thermal stability of TvGSTO1S (ΔT_d = +3.7 °C) and TvGSTO6S (ΔT_d = +3.0 °C). We chose not to consider these potential opposite effects, and the following analysis was performed using the absolute value of the detected ΔT_d ($|\Delta T_d|$).

Properties of Wood Extracts. The antimicrobial activity of the extracts was tested against a wood decaying

DOI: 10.1021/acssuschemeng.8b02636
ACS Sustainable Chem. Eng. 2018, 6, 13078−13085

Table 1. Pearson Coefficients Showing the Correlation between Variables[a]

variables	(I) *Bf*	(I) *Cp*	(I) *Pc*	$\lvert\Delta T_d\rvert$ 1	$\lvert\Delta T_d\rvert$ 2	$\lvert\Delta T_d\rvert$ 3	$\lvert\Delta T_d\rvert$ 4	$\lvert\Delta T_d\rvert$ 5	$\lvert\Delta T_d\rvert$ 6	A_P	A_R
(I) *Bf*	1	**0.805**	**0.606**	−0.199	**0.606**	−0.119	0.178	0.319	0.072	0.194	0.201
(I) *Cp*		1	**0.486**	−0.239	**0.464**	−0.067	0.303	0.248	−0.072	0.026	0.038
(I) *Pc*			1	−0.132	**0.519**	−0.029	0.167	0.225	0.041	0.034	0.005
$\lvert\Delta T_d\rvert$ 1				1	0.181	**0.730**	0.091	0.309	**0.418**	−0.088	−0.073
$\lvert\Delta T_d\rvert$ 2					1	−0.002	0.052	**0.529**	0.213	**0.347**	**0.375**
$\lvert\Delta T_d\rvert$ 3						1	0.327	0.134	**0.437**	−0.313	−0.321
$\lvert\Delta T_d\rvert$ 4							1	0.083	0.176	−0.096	−0.072
$\lvert\Delta T_d\rvert$ 5								1	−0.139	−0.137	−0.035
$\lvert\Delta T_d\rvert$ 6									1	0.265	0.195
A_P										1	**0.953**
A_R											1

[a]Values in bold have *p*-values lower than the significant threshold ($p < 0.05$) and are significantly different. Symbol (I) corresponds to the inhibition index on the studied microorganisms: *Bf* for *Bacillus fungorum*, *Cp* for *Collimonas pratensis*, and *Pc* for *Phanerochaete chrysosporium*. The absolute values of thermal shift ($\lvert\Delta T_d\rvert$) for the six isoforms TvGSTO1S (1), TvGSTO2S (2), TvGSTO3S (3), TvGSTO4S (4), TvGSTO5S (5), and TvGSTO6S (6) have been required for performing this Pearson correlation. For the phenolic content (A_P) and reductase activity (A_R), the same values were used (equivalent of gallic acid and of ascorbic acid in $\mu g\ L^{-1}$).

basidiomycete *Phanerochaete chrysosporium* and two bacterial strains isolated from degraded wood, *Collimonas pratensis* Ter91 and *Burkholderia fungorum* LMG 16225.[23,24] The three organisms were cultivated in the presence or absence of the tested wood extracts. The potential antimicrobial effect was calculated from maximal growth rates measured in the presence or absence of the tested extracts. A statistical analysis of the obtained data (Table S1) shows that these "antimicrobial" variables are significantly correlated (Table 1) with a Pearson correlation coefficient higher between both bacterial variables ($r = 0.805$, $p = 1.7 \times 10^{-8}$).

For investigating the antioxidant activity, two distinct methods were used: determination of phenolic content and reductive abilities. These "antioxidative variables" were revealed to be strongly correlated ($r = 0.953$, $p = 10^{-12}$) (Table 1).

Relationship between Thermal Responses of TvGSTOs and the Biological Properties of Wood Extract. Potential correlations between "TvGSTOS" variables (defined as the absolute value of the detected ΔT_d for a specific isoform) and antioxidative and antimicrobial variables were investigated (Table 1). No significant correlation was detected with five isoforms (TvGSTO1S, 3S, 4S, 5S, and 6S). In contrast, interactions between the "TvGSTO2S" variable and the tested wood extracts are clearly related to the chemical properties of the latter (Table 1). The "TvGSTO2S" variable is indeed correlated both to the "antioxidative variables" (phenolic content and reductase activity; $r = 0.347$, $p = 0.048$, and $r = 0.375$, $p = 0.031$, respectively) and to the "antimicrobial variables" ($r = 0.519$, $p = 0.002$; $r = 0.606$, $p = 0.001$; and $r = 0.464$, $p = 0.007$ for *P. chrysosporium*, *B. fungorum*, and *C. pratensis*, respectively) (Table 1).

A principal component (PC) analysis was also performed using all these data (Figure 1).

Three PCs explained ~69.25% of the total variance among the 32 tested extracts. Of these, the first two PCs explained ~50.76% of the total variance. The overall distribution of the wood extracts on the graph does not show a clear clustering, although all of the samples are clearly distinguishable from the control (DMSO). Briefly, the PC analysis showed that the coordinates of several wood extracts obtained with water, mix toluene/ethanol, and acetone were near among them. In contrast, it appeared that the coordinates of wood extracts

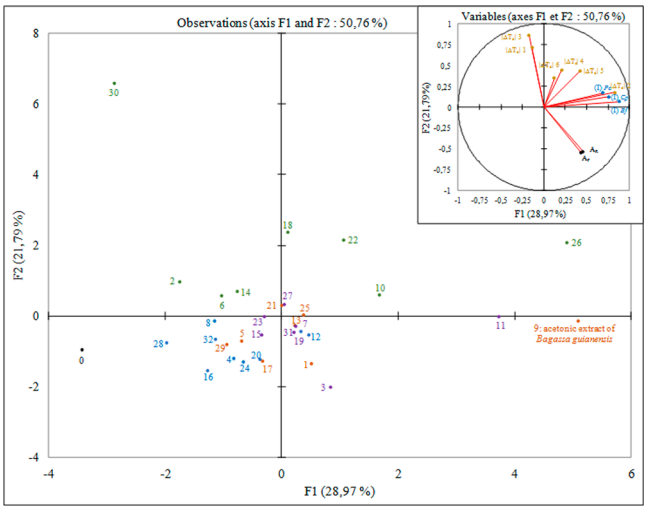

Figure 1. Principal component (PC) analysis performed using "$\lvert\Delta T_d\rvert$ TvGSTO1-6S", "antimicrobial", and "antioxidative" variables (Table S1) obtained with the following wood extracts. For each wood extract, absolute values of thermal shifts for the six isoforms were required for this PC. According to the protein (TvGSTO1-6S), the variables are represented by "$\lvert\Delta T_d\rvert$ 1", "$\lvert\Delta T_d\rvert$ 2", "$\lvert\Delta T_d\rvert$ 3", "$\lvert\Delta T_d\rvert$ 4", "$\lvert\Delta T_d\rvert$ 5", and "$\lvert\Delta T_d\rvert$ 6". The inhibition indexes on the growth of the three microorganisms were used, and the variables are represented in blue: (I) *Pc* for inhibition on the growth of *P. chrysosporium*, (I) *Cp* for *C. pratensis*, and (I) *Bf* for *B. fungorum*. Concerning both antioxidative variables, the phenolic content (A_P) and reductase activity (A_R) are symbolized in black. Each number corresponds to a wood extract (see Table S1). According to the solvent, the color is different: green for dichloromethane, orange for acetone, purple for the mix toluene/ethanol, and blue for water. The number 0 corresponds to the control condition (for dimethyl sulfoxide).

obtained with dichloromethane were different and were heterogeneously distributed. Interestingly, the acetonic and the toluene/ethanolic extracts of *Bagassa guianensis* differ from the others (Figure 1, nos. 9 and 11), displaying both antifungal and antibacterial properties and modifying the thermal stability of TvGSTO2S (ΔT_d = +5.25 °C, ΔT_d = +2.00 °C respectively).

Taken together, these data suggested that the detected interactions between wood extracts and TvGSTO2S could be used to detect molecules with biological properties. The

DOI: 10.1021/acssuschemeng.8b02636
ACS Sustainable Chem. Eng. 2018, 6, 13078−13085

acetonic extract of *Bagassa guianensis* was then chosen to focus this work on the potential interactions with TvGSTO2S.

Study of the Chemical Composition and Properties of the Acetonic Extract of *Bagassa guianensis*. The chemical composition of the acetonic extract of *Bagassa guianensis* was first analyzed by GC-MS, showing the presence of oxyresveratrol as the main product (peak at 21.82 min; Figure S1) in accordance with previous studies.[34] The other peaks (19.42, 20.81, 21.10, 22.46, and 25.72 min) revealed the presence of derivatives of oxyresveratrol: resveratrol and cyclization forms of oxyresveratrol. After separation of the extract by reversed-phase high-performance liquid chromatography (HPLC), the harvested fractions were evaporated. The fractions were solubilized in DMSO and then tested for the content of phenolic compounds, the reducing power, their antimicrobial activity (in this case, the inhibition of *Saccharomyces cerevisiae* growth rate), and their interactions with TvGSTO2S (Table S2). As shown in Figure 2, a strong correlation between the antioxidative properties of the fractions and their interactions with TvGSTO2S was observed (r = 0.957, p = 10^{-12}).

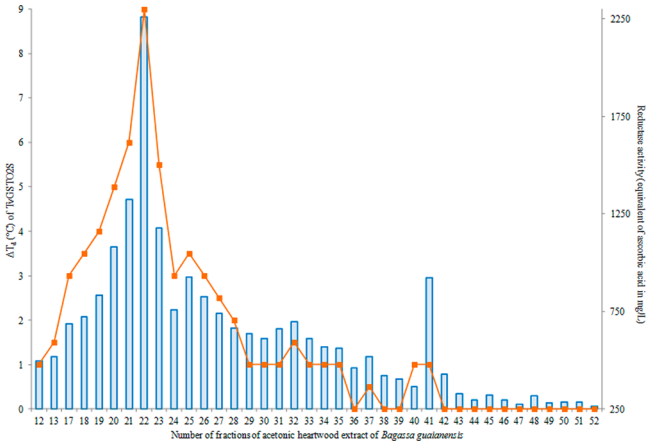

Figure 2. Thermal effects on TvGSTO2S and reductase activity of fractions from acetonic heartwood extract of *Bagassa guaianensis*. Blue bars represent the reductase activity (converted in equivalent of ascorbic acid in mg L^{-1}), and the orange line corresponds to the thermal shifts (ΔT_d, in °C) induced by each fraction.

Interactions with TvGSTO2S revealed mainly the presence of two pools of fractions centered around fractions 22 and 41, respectively, that induced an increase in the thermal stability of the protein (Figure 2). The GC-MS analysis revealed that fraction 22 mainly contained oxyresveratrol and dihydromorin and that fraction 41 contained 6-O-methyl-moracin N. All these compounds have been previously detected in *Bagassa guianensis* extract.[34] 6-O-Methyl-moracin N has been shown to exhibit antimicrobial activity, and dihydromorin shows a tyrosinase inhibitory effect.[19,35] Because of the major presence of oxyresveratrol in this extract, we chose to test the pure compound. For the next part of this work, a biochemical and structural study has been conducted to investigate the interactions between TvGSTO2S and oxyresveratrol at the molecular level.

Characterization of the Interaction between TvGSTO2S and Oxyresveratrol. To better understand the effect of oxyresveratrol on the denaturation temperature (ΔT_d) of TvGSTO2S, we tested several concentrations of stilbene with the same method (Figure 3).

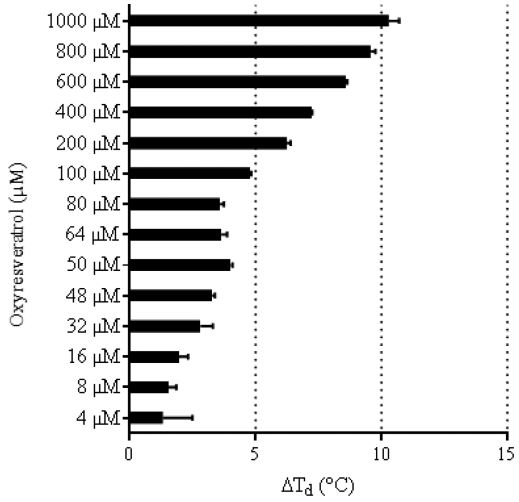

Figure 3. Stabilizing effects of oxyresveratrol on TvGSTO2S. Thermal shifts (ΔT_d) are given in °C. For each tested concentration of oxyresveratrol, the final concentration of protein was 10 μM.

ΔT_d of TvGSTO2S is significantly modified with at least 8 μM oxyresveratrol (ΔT_d = +1.55 °C). This approach did not allow an accurate determination of the apparent affinity of TvGSTO2S for oxyresveratrol.[36] Then, an enzymatic approach was performed using the ability of TvGSTO2S to transfer glutathione on PEITC. In the absence of oxyresveratrol, the following parameters have been obtained: K_M = 29.71 ± 2.84 μM and k_{cat} = 12.01 ± 0.26 s^{-1}, confirming the ability of TvGSTO2S to efficiently transfer glutathione on this substrate.[16] This activity is strongly inhibited in the presence of oxyresveratrol (K_I of 3.79 ± 1.51 μM), confirming that the stilbene is able to bind to the studied protein. Next in the study of interactions between TvGSTO2S and oxyresveratrol, an association constant k_{on} of 141 ± 18 M^{-1} s^{-1} was determined using the switchSENSE technology (Figure S2). However, the dissociation constant k_{off} was not determined as the oxyresveratrol and the protein formed a highly stable complex (no dissociation observed, Figure S2). In addition, no modification of the stilbene mediated by the TvGSTO2S was observed in the presence or absence of glutathione, suggesting that the stilbene is not a substrate for the protein.

The interactions between TvGSTO2S and oxyresveratrol were also studied at the atomic level. The TvGSTO2S crystal structure was solved at 2.19 Å (Table S5). The protein adopts a dimeric arrangement with its monomers exhibiting the characteristic traits of the cytosolic GST fold (Figure 4).

Besides its conserved two-domain organization (N-terminal domain, $\beta1\alpha1\beta2\alpha2\beta3\beta4\alpha3$, residues Cys3-Ala95; C-terminal domain, $\alpha4\alpha5\alpha6\alpha6'\alpha7\alpha8\alpha9$, Lys96-Arg236), TvGSTO2S shows the specificities of the fungal type-III Omega class, an extended loop between strands $\beta3$ and $\beta4$, a potential catalytic serine at the N-terminus of helix $\alpha1$, and an additional helix $\alpha6'$.[17] TvGSTO2S shares the same overall structure as its previously studied isoforms TvGSTO3S (rmsd of 1.366 Å for 416 aligned Cα, PDB ID: 6F43)[17] and TvGSTO6S (rmsd of 2.223 Å for 460 aligned Cα, PDB ID: 6F70).[17]

The TvGSTO2S crystal soaked with oxyresveratrol resulted in a structure without major conformational changes with

DOI: 10.1021/acssuschemeng.8b02636
ACS Sustainable Chem. Eng. 2018, 6, 13078−13085

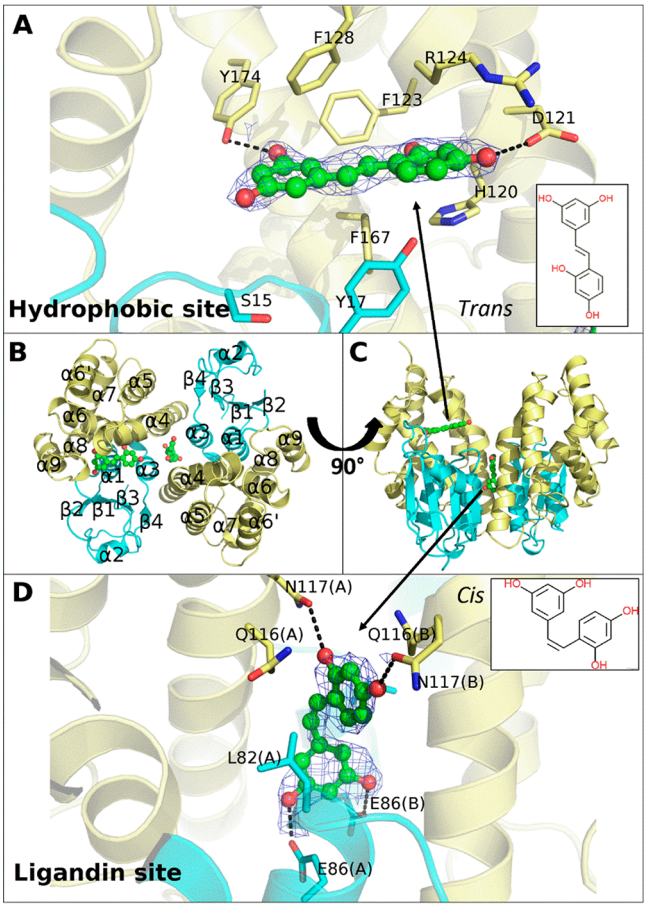

Figure 4. Crystal structure of TvGSTO2S complexed with *trans*- and *cis*-oxyresveratrol. (A) Oxyresveratrol in *trans* configuration bound to the TvGSTO2S hydrophobic site. (B,C) Overall views of TvGSTO2S structure complexed with *trans*- and *cis*-oxyresveratrol. Secondary structure elements are displayed in (B). N-terminal domain is colored cyan, and C-terminal domain is colored pale yellow. (D) Oxyresveratrol in *cis* configuration bound to the TvGSTO2S ligandin site at the dimer interface. Topological structures of *trans*- and *cis*-oxyresveratrol are shown in corresponding panels. Ligands are represented as green sticks and spheres. Polar interactions are represented as dashed lines. 2mFo-DFc omit maps calculated by PHENIX are displayed at 1.0σ around ligands.

respect to the apo form. However, two main continuous regions were detected in the Fo-Fc electron density map corresponding to two oxyresveratrol molecules. The first one binds in the hydrophobic site (H site) of monomer B of TvGSTO2S (Figure 4). In this case, the ligand is in a native *trans* configuration and is stabilized in a slit formed by the hydrophobic side chains of Phe123, Phe128, and Phe167. Oxyresveratrol molecule in *trans* configuration interacts by H-bonding with Asp121 and Tyr174 from helix α4 and α6, respectively. The second molecule of oxyresveratrol binds in the site known as ligandin site (L site) at the TvGSTO2S dimer interface. Here, it adopts a *cis* configuration according to the aromatic groups positioned on the same side of the central double bond (Figure 4). Stilbenes, including oxyresveratrol, are known to undergo *trans*/*cis* isomerization, which can be achieved by light irradiation.[37] This likely occurred in our experiment during the drying step before crystal dry-soaking. Oxyresveratrol molecule in *cis* configuration is well stabilized by four H-bonds established between the ligand hydroxy groups and the side chains of Glu86 (monomer A), Glu86 (B), Asn117 (A), and Asn117 (B) located at the dimer interface. These structural results support the strong interaction measured between TvGSTO2S and oxyresveratrol and suggest that this GST is able to interact with both *cis* and *trans* isomers at different sites.

DISCUSSION

Forests, and in particular tropical forests, are reservoirs of amazing biodiversity, where trees play a major role in interacting with a large number of biological partners. These interactions are often due to the exchange of molecular signals. The molecular diversity of the involved compounds is linked to the extraordinary variability of plant secondary metabolism. For centuries, humans have used this diversity to obtain compounds or mixtures of compounds with antimicrobial and insecticidal activity. This is the case, for instance, of wood extractives. Depending on the considered species, these compounds may have functions in wood durability and may also exhibit antimicrobial and insecticidal activities. Numerous studies have indeed been devoted to the identification and characterization of these molecules.[1,3,38−40] On another hand, the wood decayers, microorganisms and insects, have developed efficient detoxification systems to deal with these compounds and also to use wood as a source of nutriments. From comparative genomic and previously from functional studies, it appears that these systems are mainly constituted of multigenic families.[5,7,41] The resulting proteins are involved in either oxidation of wood metabolites (e.g., cytochrome P450 monooxygenases) or a decrease of their chemical reactivity by addition of sugars or glutathione. These latest reactions are catalyzed by glycosyl or glutathione transferases depending on the chemical nature of the considered adduct.

The relationship between both diversities, i.e., wood extractives and detoxification enzymes, seems obvious and suggests that the latter could be used to study the chemical diversity of wood extracts and then to identify molecules that possess interesting properties for industry such as antimicrobial or antioxidative properties. In the present study, we have validated this hypothesis studying interactions between six GSTs from the white-rot *Trametes versicolor* and a library of wood extracts. The thermal shift assay has been used; this method allows fast screening of hundreds of samples using a small amount (μg) of extracts. The obtained results demonstrated that TvGSTOSs were more prone to interact with hydrophobic compounds because dichloromethane extracts induced the highest shifts of the thermal denaturation temperatures. The six proteins show a specific pattern of interactions as previously shown with libraries of molecules.[17] Interestingly, the thermal stability of TvGSTO2S in the presence of the extracts is significantly correlated to antimicrobial and antioxidative properties of the latter. The interaction could occur at different sites of the protein. A *trans*-oxyresveratrol molecule occupies the active site (H-site), and a *cis*-oxyresveratrol molecule occupies the dimer interface (L-site). These two sites were already described as binding sites for noncatalytic ligand in TvGSTOs.[17] These observations agree with the assumed ligandin function of GSTs that can facilitate the sequestration and transport of hydrophobic molecules.[42,43] This ligandin property could be due to particular sites found at the dimer interface as demonstrated here for TvGSTO2S.[44,45] The presence of this L-site increases in this way the number of potential interactions of GSTs with

DOI: 10.1021/acssuschemeng.8b02636
ACS Sustainable Chem. Eng. 2018, 6, 13078−13085

ligands. In accordance with the obtained biochemical data, binding of oxyresveratrol at the H-site could be responsible for the inhibition of TvGSTO2S glutathionylation activity. Nevertheless, further experiments are required to evaluate the affinity of the L-site for oxyresveratrol and the consequences of this binding on the activity of the enzyme.

As detoxification enzymes, we postulated that the substrates or ligands of GSTs could have interesting properties with potential industrial applications. This is the case for oxyresveratrol, which has been studied for its multiple properties such as anti-inflammatory activity,[46] antioxidative activity,[47] and antibacterial activity.[48] Through the example of TvGSTO2S and oxyresveratrol, the obtained data support the hypothesis that the detoxification systems of wood decayers, and in particular glutathione transferases, could be used to identify and characterize wood molecules with potential interest. At the same time, this approach should give insights on the chemical environment encountered by the studied organisms and then increase our understanding of their adaptation to their trophic features.

■ ASSOCIATED CONTENT

Supporting Information

The Supporting Information is available free of charge on the ACS Publications website at DOI: 10.1021/acssuschemeng.8b02636.

Glutathione transferases, antimicrobial and antioxidative variables obtained with wood extracts; TvGSTO2S, antimicrobial, and antioxidative variables obtained with fractionated *Bagassa guianensis* acetonic extract; diffraction and refinement statistics; GS-MS analysis of acetonic extract of *Bagassa guianensis*; and real-time molecular interaction between TvGSTO2S and oxyresveratrol determined by switchSENSE analysis (PDF)

■ AUTHOR INFORMATION

Corresponding Author

*E-mail: eric.gelhaye@univ-lorraine.fr.

ORCID

Thomas Perrot: 0000-0002-5592-7941

Author Contributions

‖T.P. and M.S. contributed equally to this work.

Author Contributions

E.G., C.D., F.F., and N.A. developed the concept and supervised this study. T.P., M.S., S.D., M.M.R., F.S., R.S., and G.S. performed the experiments and interpreted the data. All the authors participated in manuscript writing. E.G., C.D., P.G., and N.A. acquired the funding. All authors read and approved the final manuscript.

Funding

This study was funded by the French National Research Agency (ANR-11-LAS-0002−01), the Centre National de la Recherche Scientifique, the University of Lorraine, and the Région Grand Est (MS and TP Grants, PEPS-Mirabelle 2016, CPER 2014−2020, Program "Equipement mi-lourd 2016"). The authors acknowledge financial support from the "Impact Biomolecules" project of the "Lorraine Université d'Excellence" (Investissements d'avenir−ANR).

Notes

The authors declare no competing financial interest.

■ ACKNOWLEDGMENTS

We thank Solène Telliez, Tiphaine Dhalleine, and Sandrine Mathiot for technical assistance. We thank Sophie Mieszkin for helpful discussion concerning the bacterial strains. A sincere thank you to Jean-Pierre Jacquot for constructive criticism of the manuscript. The authors thank ESRF for beamtime and the staff of beamline BM30A for data collections. The authors appreciated the access to the "Plateforme de mesures de diffraction X" of the University of Lorraine with crystal testing.

■ REFERENCES

(1) Anouhe, J.-B. S.; Adima, A. A.; Niamké, F. B.; Stien, D.; Amian, B. K.; Blandinières, P.-A.; Virieux, D.; Pirat, J.-L.; Kati-Coulibaly, S.; Amusant, N. Dicorynamine and Harmalan-N-Oxide, Two New β-Carboline Alkaloids from *Dicorynia guianensis* Amsh Heartwood. *Phytochem. Lett.* **2015**, *12*, 158−163.

(2) Rodrigues, A. M. S.; Theodoro, P. N. E. T.; Eparvier, V.; Basset, C.; Silva, M. R. R.; Beauchêne, J.; Espíndola, L. S.; Stien, D. Search for Antifungal Compounds from the Wood of Durable Tropical Trees. *J. Nat. Prod.* **2010**, *73* (10), 1706−1707.

(3) Valette, N.; Perrot, T.; Sormani, R.; Gelhaye, E.; Morel-Rouhier, M. Antifungal Activities of Wood Extractives. *Fungal Biol. Rev.* **2017**, *31* (3), 113−123.

(4) Frankó, B.; Carlqvist, K.; Galbe, M.; Lidén, G.; Wallberg, O. Removal of Water-Soluble Extractives Improves the Enzymatic Digestibility of Steam-Pretreated Softwood Barks. *Appl. Biochem. Biotechnol.* **2018**, *184* (2), 599−615.

(5) Morel, M.; Meux, E.; Mathieu, Y.; Thuillier, A.; Chibani, K.; Harvengt, L.; Jacquot, J.-P.; Gelhaye, E. Xenomic Networks Variability and Adaptation Traits in Wood Decaying Fungi. *Microb. Biotechnol.* **2013**, *6* (3), 248−263.

(6) Riley, R.; Salamov, A. A.; Brown, D. W.; Nagy, L. G.; Floudas, D.; Held, B. W.; Levasseur, A.; Lombard, V.; Morin, E.; Otillar, R.; et al. Extensive Sampling of Basidiomycete Genomes Demonstrates Inadequacy of the White-Rot/Brown-Rot Paradigm for Wood Decay Fungi. *Proc. Natl. Acad. Sci. U. S. A.* **2014**, *111* (27), 9923−9928.

(7) Nagy, L. G.; Riley, R.; Bergmann, P. J.; Krizsán, K.; Martin, F. M.; Grigoriev, I. V.; Cullen, D.; Hibbett, D. S. Genetic Bases of Fungal White Rot Wood Decay Predicted by Phylogenomic Analysis of Correlated Gene-Phenotype Evolution. *Mol. Biol. Evol.* **2017**, *34* (1), 35−44.

(8) Rane, R. V.; Walsh, T. K.; Pearce, S. L.; Jermiin, L. S.; Gordon, K. H.; Richards, S.; Oakeshott, J. G. Are Feeding Preferences and Insecticide Resistance Associated with the Size of Detoxifying Enzyme Families in Insect Herbivores? *Curr. Opin. Insect Sci.* **2016**, *13*, 70−76.

(9) Capolupo, M.; Valbonesi, P.; Kiwan, A.; Buratti, S.; Franzellitti, S.; Fabbri, E. Use of an Integrated Biomarker-Based Strategy to Evaluate Physiological Stress Responses Induced by Environmental Concentrations of Caffeine in the Mediterranean Mussel *Mytilus galloprovincialis*. *Sci. Total Environ.* **2016**, *563*−*564*, 538−548.

(10) Hollman, A. L.; Tchounwou, P. B.; Huang, H.-C. The Association between Gene-Environment Interactions and Diseases Involving the Human GST Superfamily with SNP Variants. *Int. J. Environ. Res. Public Health* **2016**, *13* (4), 379.

(11) Mohanty, D.; Samanta, L. Multivariate Analysis of Potential Biomarkers of Oxidative Stress in *Notopterus notopterus* Tissues from Mahanadi River as a Function of Concentration of Heavy Metals. *Chemosphere* **2016**, *155*, 28−38.

(12) Roret, T.; Thuillier, A.; Favier, F.; Gelhaye, E.; Didierjean, C.; Morel-Rouhier, M. Evolutionary Divergence of Ure2pA Glutathione Transferases in Wood Degrading Fungi. *Fungal Genet. Biol.* **2015**, *83*, 103−112.

(13) Meux, E.; Morel, M.; Lamant, T.; Gérardin, P.; Jacquot, J.-P.; Dumarçay, S.; Gelhaye, E. New Substrates and Activity of *Phanerochaete chrysosporium* Omega Glutathione Transferases. *Biochimie* **2013**, *95* (2), 336−346.

DOI: 10.1021/acssuschemeng.8b02636
ACS Sustainable Chem. Eng. 2018, 6, 13078−13085

(14) Mathieu, Y.; Prosper, P.; Favier, F.; Harvengt, L.; Didierjean, C.; Jacquot, J.-P.; Morel-Rouhier, M.; Gelhaye, E. Diversification of Fungal Specific Class a Glutathione Transferases in Saprotrophic Fungi. *PLoS One* **2013**, *8* (11), e80298.
(15) Marinović, M.; Nousiainen, P.; Dilokpimol, A.; Kontro, J.; Moore, R.; Sipilä, J.; de Vries, R. P.; Mäkelä, M. R.; Hildén, K. Selective Cleavage of Lignin *β*-O-4 Aryl Ether Bond by *β*-Etherase of the White-Rot Fungus *Dichomitus squalens*. *ACS Sustainable Chem. Eng.* **2018**, *6* (3), 2878−2882.
(16) Deroy, A.; Saiag, F.; Kebbi-Benkeder, Z.; Touahri, N.; Hecker, A.; Morel-Rouhier, M.; Colin, F.; Dumarcay, S.; Gérardin, P.; Gelhaye, E. The GSTome Reflects the Chemical Environment of White-Rot Fungi. *PLoS One* **2015**, *10* (10), e0137083.
(17) Schwartz, M.; Perrot, T.; Aubert, E.; Dumarçay, S.; Favier, F.; Gérardin, P.; Morel-Rouhier, M.; Mulliert, G.; Saiag, F.; Didierjean, C.; et al. Molecular Recognition of Wood Polyphenols by Phase II Detoxification Enzymes of the White Rot *Trametes versicolor*. *Sci. Rep.* **2018**, *8* (1), 8472.
(18) Carlson, A.; Justo, A.; Hibbett, D. S. Species Delimitation in *Trametes*: A Comparison of ITS, RPB1, RPB2 and TEF1 Gene Phylogenies. *Mycologia* **2014**, *106* (4), 735−745.
(19) Royer, M.; Rodrigues, A. M. S.; Herbette, G.; Beauchêne, J.; Chevalier, M.; Hérault, B.; Thibaut, B.; Stien, D. Efficacy of *Bagassa guianensis* Aubl. Extract against Wood Decay and Human Pathogenic Fungi. *Int. Biodeterior. Biodegrad.* **2012**, *70*, 55−59.
(20) Langer, A.; Kaiser, W.; Svejda, M.; Schwertler, P.; Rant, U. Molecular Dynamics of DNA-Protein Conjugates on Electrified Surfaces: Solutions to the Drift-Diffusion Equation. *J. Phys. Chem. B* **2014**, *118* (2), 597−607.
(21) Joubert, A.; Calmes, B.; Berruyer, R.; Pihet, M.; Bouchara, J.-P.; Simoneau, P.; Guillemette, T. Laser Nephelometry Applied in an Automated Microplate System to Study Filamentous Fungus Growth. *BioTechniques* **2010**, *48* (5), 399−404.
(22) Tien, M.; Kirk, T. K. Lignin-Degrading Enzyme from the Hymenomycete *Phanerochaete chrysosporium* Burds. *Science* **1983**, *221* (4611), 661−663.
(23) Hervé, V.; Le Roux, X.; Uroz, S.; Gelhaye, E.; Frey-Klett, P. Diversity and Structure of Bacterial Communities Associated with *Phanerochaete chrysosporium* during Wood Decay. *Environ. Microbiol.* **2014**, *16* (7), 2238−2252.
(24) Hervé, V.; Ketter, E.; Pierrat, J.-C.; Gelhaye, E.; Frey-Klett, P. Impact of *Phanerochaete chrysosporium* on the Functional Diversity of Bacterial Communities Associated with Decaying Wood. *PLoS One* **2016**, *11* (1), e0147100.
(25) Oyaizu, M. Studies on Products of Browning Reaction. *Eiyogaku Zasshi* **1986**, *44* (6), 307−315.
(26) Yen, G.-C.; Chen, H.-Y. Antioxidant Activity of Various Tea Extracts in Relation to Their Antimutagenicity. *J. Agric. Food Chem.* **1995**, *43* (1), 27−32.
(27) Canabady-Rochelle, L. L. S.; Harscoat-Schiavo, C.; Kessler, V.; Aymes, A.; Fournier, F.; Girardet, J.-M. Determination of Reducing Power and Metal Chelating Ability of Antioxidant Peptides: Revisited Methods. *Food Chem.* **2015**, *183*, 129−135.
(28) Taga, M. S.; Miller, E. E.; Pratt, D. E. Chia Seeds as a Source of Natural Lipid Antioxidants. *J. Am. Oil Chem. Soc.* **1984**, *61* (5), 928−931.
(29) Kabsch, W. XDS. *Acta Crystallogr., Sect. D: Biol. Crystallogr.* **2010**, *66* (Pt 2), 125−132.
(30) Winn, M. D.; Ballard, C. C.; Cowtan, K. D.; Dodson, E. J.; Emsley, P.; Evans, P. R.; Keegan, R. M.; Krissinel, E. B.; Leslie, A. G. W.; McCoy, A.; et al. Overview of the CCP4 Suite and Current Developments. *Acta Crystallogr., Sect. D: Biol. Crystallogr.* **2011**, *67* (Pt 4), 235−242.
(31) Adams, P. D.; Afonine, P. V.; Bunkóczi, G.; Chen, V. B.; Davis, I. W.; Echols, N.; Headd, J. J.; Hung, L.-W.; Kapral, G. J.; Grosse-Kunstleve, R. W.; et al. PHENIX: A Comprehensive Python-Based System for Macromolecular Structure Solution. *Acta Crystallogr., Sect. D: Biol. Crystallogr.* **2010**, *66* (Pt 2), 213−221.
(32) Emsley, P.; Cowtan, K. Coot: Model-Building Tools for Molecular Graphics. *Acta Crystallogr., Sect. D: Biol. Crystallogr.* **2004**, *60* (Pt 12 Pt 1), 2126−2132.
(33) Davis, I. W.; Murray, L. W.; Richardson, J. S.; Richardson, D. C. MOLPROBITY: Structure Validation and All-Atom Contact Analysis for Nucleic Acids and Their Complexes. *Nucleic Acids Res.* **2004**, *32* (Web Server issue), W615−619.
(34) Royer, M.; Herbette, G.; Eparvier, V.; Beauchêne, J.; Thibaut, B.; Stien, D. Secondary Metabolites of *Bagassa guianensis* Aubl. Wood: A Study of the Chemotaxonomy of the Moraceae Family. *Phytochemistry* **2010**, *71* (14−15), 1708−1713.
(35) Hu, S.; Zheng, Z.; Zhang, X.; Chen, F.; Wang, M. Oxyresveratrol and Trans-Dihydromorin from the Twigs of *Cudrania tricuspidata* as Hypopigmenting Agents against Melanogenesis. *J. Funct. Foods* **2015**, *13*, 375−383.
(36) Vivoli, M.; Novak, H. R.; Littlechild, J. A.; Harmer, N. J. Determination of Protein-Ligand Interactions Using Differential Scanning Fluorimetry. *J. Visualized Exp.* **2014**, *91*, 1.
(37) Maafi, M.; Al-Qarni, M. A. Φ-Order Spectrophotokinetic Characterisation and Quantification of Trans-Cis Oxyresveratrol Reactivity, Photodegradation and Actinometry. *Spectrochim. Acta, Part A* **2018**, *188*, 64−71.
(38) Bossu, J.; Beauchêne, J.; Estevez, Y.; Duplais, C.; Clair, B. New Insights on Wood Dimensional Stability Influenced by Secondary Metabolites: The Case of a Fast-Growing Tropical Species *Bagassa guianensis* Aubl. *PLoS One* **2016**, *11* (3), e0150777.
(39) Doussot, F.; De Jéso, B.; Quideau, S.; Pardon, P. Extractives Content in Cooperage Oak Wood during Natural Seasoning and Toasting; Influence of Tree Species, Geographic Location, and Single-Tree Effects. *J. Agric. Food Chem.* **2002**, *50* (21), 5955−5961.
(40) Rodrigues, A. M. S.; Amusant, N.; Beauchêne, J.; Eparvier, V.; Leménager, N.; Baudassé, C.; Espindola, L. S.; Stien, D. The Termiticidal Activity of *Sextonia rubra* (Mez) van Der Werff (*Lauraceae*) Extract and Its Active Constituent Rubrynolide. *Pest Manage. Sci.* **2011**, *67* (11), 1420−1423.
(41) Syed, K.; Shale, K.; Pagadala, N. S.; Tuszynski, J. Systematic Identification and Evolutionary Analysis of Catalytically Versatile Cytochrome P450 Monooxygenase Families Enriched in Model Basidiomycete Fungi. *PLoS One* **2014**, *9* (1), e86683.
(42) Cummins, I.; Dixon, D. P.; Freitag-Pohl, S.; Skipsey, M.; Edwards, R. Multiple Roles for Plant Glutathione Transferases in Xenobiotic Detoxification. *Drug Metab. Rev.* **2011**, *43* (2), 266−280.
(43) Zhao, J. Flavonoid Transport Mechanisms: How to Go, and with Whom. *Trends Plant Sci.* **2015**, *20* (9), 576−585.
(44) Brock, J.; Board, P. G.; Oakley, A. J. Structural Insights into Omega-Class Glutathione Transferases: A Snapshot of Enzyme Reduction and Identification of a Non-Catalytic Ligandin Site. *PLoS One* **2013**, *8* (4), e60324.
(45) Ahmad, L.; Rylott, E. L.; Bruce, N. C.; Edwards, R.; Grogan, G. Structural Evidence for Arabidopsis Glutathione Transferase AtGSTF2 Functioning as a Transporter of Small Organic Ligands. *FEBS Open Bio* **2017**, *7* (2), 122−132.
(46) Chen, Y.-C.; Tien, Y.-J.; Chen, C.-H.; Beltran, F. N.; Amor, E. C.; Wang, R.-J.; Wu, D.-J.; Mettling, C.; Lin, Y.-L.; Yang, W.-C. *Morus alba* and Active Compound Oxyresveratrol Exert Anti-Inflammatory Activity via Inhibition of Leukocyte Migration Involving MEK/ERK Signaling. *BMC Complementary Altern. Med.* **2013**, *13*, 45.
(47) Lorenz, P.; Roychowdhury, S.; Engelmann, M.; Wolf, G.; Horn, T. F. W. Oxyresveratrol and Resveratrol Are Potent Antioxidants and Free Radical Scavengers: Effect on Nitrosative and Oxidative Stress Derived from Microglial Cells. *Nitric Oxide* **2003**, *9* (2), 64−76.
(48) Joung, D.-K.; Mun, S.-H.; Choi, S.-H.; Kang, O.-H.; Kim, S.-B.; Lee, Y.-S.; Zhou, T.; Kong, R.; Choi, J.-G.; Shin, D.-W.; et al. Antibacterial Activity of Oxyresveratrol against Methicillin-Resistant *Staphylococcus aureus* and Its Mechanism. *Exp. Ther. Med.* **2016**, *12* (3), 1579−1584.

DOI: 10.1021/acssuschemeng.8b02636
ACS Sustainable Chem. Eng. 2018, 6, 13078−13085